

Method

Ultraviolet-induced fluorescent imaging for millipede taxonomy

Paul Marek ‡, §

‡ Virginia Polytechnic Institute and State University, Blacksburg, United States of America

§ Virginia Tech, Blacksburg, United States of America

Corresponding author: Paul Marek (paulemarek@gmail.com)

Reviewable v1

Received: 03 Jul 2017 | Published: 04 Jul 2017

Citation: Marek P (2017) Ultraviolet-induced fluorescent imaging for millipede taxonomy. Research Ideas and Outcomes 3: e14850. <https://doi.org/10.3897/rio.3.e14850>

Abstract

Fluorescent imaging has been traditionally applied to cell biology, and more recently to entomology to capture microscopic images of insect anatomy. However, the technique has not been applied to the study of millipedes, most of which autofluoresce as a result of endogenous fluorescent molecules in their cuticle such as pterins and coproporphyrins. This study compares commercially available ultraviolet light sources for fluorescent photography of millipedes for the documentation of anatomical structures. Millipedes that were most strongly fluorescent were those in the order Polydesmida, and produced the brightest fluorescence that was most easily photographed using this technique. However, millipedes of the orders Spirobolida and Siphonophorida were also fluorescent and produced a bright blue visible emission. The best quality images were those obtained with a modified flash that produced the highest intensity and shortest wavelength ultraviolet light.

Keywords

Diplopoda, Motyxia, systematics, Xystodesmidae

Introduction

Millipede taxonomy has thrived with the introduction of modern laboratory techniques such as DNA sequencing, scanning electron microscopy, micro-computed tomography, and high depth of field photography. Fluorescence microscopy is one technique that has recently been introduced for visualizing and capturing morphological images in taxonomy. Fluorescence is an optical phenomenon whereby shorter wavelength light (typically ultraviolet) is absorbed by a material and re-emitted at a longer wavelength. The conversion takes place through relaxation of an excited singlet state orbital electron in a fluorescent molecule to a ground state thereby emitting a lower energy and longer wavelength photon (Johnsen 2012). Though initially popularized at the cellular scale for capturing detailed images of molecules tagged with green fluorescent protein (GFP), the technique has been adapted for entomological taxonomy for use at the millimeter scale (Lee et al. 2009, Pearsons et al. 2017). While some non-fluorescent arthropods require treatment of their cuticle with a fluorescent dye prior to imaging, other species exhibit endogenous fluorescence (i.e., autofluorescence) as a result of the inherent molecular composition of the cuticle. For example, the millipede *Motyxia sequoiae* (Loomis and Davenport, 1951) is fluorescent and produces a blue light (500 nm) when illuminated with ultraviolet (UV) light with a wavelength of 350 nm (Kuse et al. 2001). The widely introduced invasive species, *Oxidus gracilis* (C.L. Koch, 1847), is weakly fluorescent and the cuticle-lined exocrine glands are observable with confocal microscopy (Pearsons et al. 2017). While a different light phenomenon than fluorescence, all millipedes of the genus *Motyxia* are simultaneously bioluminescent whereby light is generated biochemically without primary radiation of UV light (Marek and Moore 2015). It has been empirically demonstrated that bioluminescence in *M. sequoiae* serves as a nocturnal aposematic signal, while the role of fluorescence in millipedes is uncertain and has not been empirically evaluated (Marek et al. 2011). In other plants and animals, fluorescence serves a diversity of roles ranging from sexual communication to attracting pollinators (Marshall and Johnsen 2017). The bioluminescence of *M. sequoiae* possesses a wavelength maximum of 495 nm, while the fluorescence (illuminated with 350 nm ultraviolet light) is spectrally similar with a peak wavelength of 500 nm. The Stokes shift of the fluorescence of *Motyxia*, which explains the difference in absorption versus emission wavelength maxima of fluorescence, is 150 nm (i.e., from 350 – 500 nm). In addition to the nine species of *Motyxia*, other species of its tribe Xystocheirini fluoresce at a similar wavelength upon radiation with UV light; however, these species are not bioluminescent. Species of Polydesmida, including many species of Xystodesmidae and Polydesmidae, and some taxa in the Spirobolida, are fluorescent. The bioluminescent millipede *Paraspirobolus lucifugus* (Gervais, 1836), order Spirobolida, is also notably fluorescent (Oba et al. 2011, Rosenberg and Meyer-Rochow 2009). What predicts the phylogenetic distribution of fluorescence is uncertain. Co-occurrence of fluorescence and bioluminescence is known in many deep sea organisms where the two phenomena are often biochemically linked for the production of light whereby the fluorescent material is the ultimate light emitter through energy transfer (Shimomura 2006). In this case, the fluorophore, which is the fluorescent molecule, can alter the final wavelength that is ultimately emitted via energy reduction described by

Stokes shift. While many diplopod species readily produce visible fluorescence with illumination of a low-power UV lamp, other species are non-fluorescent under the same light source. The molecular source of fluorescence in millipedes may vary, but in *M. sequoiae* and the closely related xystodesmid species *Parafontaria laminata* (Attems, 1909), the fluorophore has been identified as a pterin molecule (Kuse et al. 2001, Kuse et al. 2010). The fluorescent pterin in *P. laminata* is pterin-6-carboxylic acid, while *M. sequoiae* possesses two pterins: 7,8-dihydropterin-6-carboxylic acid and pterin-6-carboxylic acid (Oba et al. 2017). Coproporphyrin is another fluorescent molecule that has been extracted from the cuticle of the polydesmidan millipede, *Polydesmus angustus* Latzel, 1884 (Needham 1968).

During research on *Motyxia* species in California, and while photographing xystocheirine millipedes in the dark illuminated with handheld fluorescent lamps, the resulting images were frequently observed to be in sharp focus and striking in appearance due to the juxtaposition of the blue fluorescence against the dark background of the forest at night. The fluorescence of heavily calcified cuticle, antennae, legs and other regions with several layers of exoskeleton produced exceptionally sharp images. Since the heavily sclerotized gonopods are of primary interest in diplopod taxonomy, and are traditionally challenging to visualize due to their small size, experiments were conducted with several commercially available ultraviolet light sources and color filters to identify a suitable set of parameters for consistently taking high quality images of these features. In this study, I describe the experiments conducted to develop several inexpensive techniques for laboratory imaging of millipedes using UV induced fluorescence.

Materials and methods

Live specimens were collected and prepared according to Means et al. (2015). The gonopods (anterior pair of legs on the seventh body ring that in males have been modified into sperm-transfer devices) were dissected with a needle and mounted in a watch-glass atop a 2-mm layer of glycerin/alcohol-based hand sanitizer to stabilize and reduce shake, and then were completely covered with 80% ethanol for photography. The following taxa were imaged: *Siphonacme lytoni* Cook & Loomis, 1928 (Siphonophorida, Siphonophoridae); *Tylobolus uncigerus* (Wood, 1864) (Spirobolida, Spirobolidae); *Pseudopolydesmus canadensis* (Newport, 1814) (Polydesmida, Polydesmidae); *Brachoria sheari* Marek, 2010 (Polydesmida, Xystodesmidae); *Motyxia tularea tularea* (Chamberlin, 1941); and *M. sequoiae* (Polydesmida, Xystodesmidae).

Photographs were taken with a Canon 6D dSLR camera with a 65 mm Canon MP-E macro lens mounted on a Passport II Portable Digital Imaging System (Canon, Tokyo, Japan; Visionary Digital, Charlottesville, USA). The Passport II includes a motor-based drive system to vary the focal distance for image stacking in Helicon Focus (HeliconSoft, Kharkiv, Ukraine). Images were captured at the shutter speed, aperture, and other settings described in Table 1. Specimens were illuminated for photography with a modified Canon 199A flash (see modification description below) and commercially available ultraviolet light-

emitting diodes (Super Bright LEDs Inc., St. Louis, USA). The left gonopod of *B. sheari* was used as a standard structure to compare UV light sources, and the modified Canon flash was used as a standard light source to compare fluorescent imaging amongst millipede taxa.

Table 1. Illumination sources assessed in the study. Images of light sources shown in Suppl. material 1.			
Illumination source	Maximum wavelength (nm)	Comments	Power, shutter speed, f-stop
Canon 199A modified flash, part: 199A	350	Modified stock flash. Images sharp, lacking purple or blue halos. Individual seta discernable. Dark background. Transparent, prostatic sperm groove visible.	6V and required 4 AA batteries. Shutter: 1/125 s f-stop: 5.6
Halo UV-blacklight, 80 mm, part: AE80-UV48-BK	450	80 mm diameter circular array of 48 SMD LEDs suspended 1 cm above the watch glass. Image of the gonopod was dominated by a blue halo concealing the outline of the setae. Medium transparency, prostatic sperm groove on apex somewhat visible.	12V, no resistor required. Shutter: 2 s f-stop: 2.8
Halo UV-blacklight, 100 mm, part: AE100-UV33	450	100 mm diameter circular array of 33 SMD LEDs. Light suspended 6 cm above the watch glass. Gonopod image dominated with a purple halo concealing the outline of the seta. Medium transparency, prostatic sperm groove on apex somewhat visible.	12V, no resistor required. Shutter: 1.5 s f-stop: 2.8
Three-array square SMD LED, part: LBM-UV 3SMB	395	Three SMD LEDs arranged in a triangle. Light was oriented 6 cm from the specimen and at 30°. Gonopod image dominated with a blue halo that obscured setae. Several purple glare spots on the gonopod apex concealed the surface appearance. Lacking transparency.	12V, no resistor required. Shutter: 2 s f-stop: 2.8
High power SMD LED, part: UV-1W-394	394	Light composed of a single high-power SMD LED requiring a heatsink. Prefemoral setae concealed behind purple halo. Broad spectrum light, produces some white light. Lacking transparency	3.4V and required a resistor and heatsink. Shutter: 1.5 s f-stop: 2.8
High power SMD LED starlight, part: PG1C-1LLS-Q3	400	Light composed of a single high-power SMD LED requiring a heatsink. Contacts difficult to solder. Quickly smoked and melted without capturing an image.	3.5V and required a resistor and heatsink. Shutter: N/A f-stop: N/A
5 mm LED, part: RL5-UV0315-380	380	Light composed of a single 5 mm LED. Prefemoral setae concealed behind dark purple halo. Medium transparency, prostatic groove on apex somewhat visible.	3.5V and required a resistor. Shutter: 1 s f-stop: 2.8

5 mm LED, radial, part: RL5-UV0315-380	380	Light composed of three 5-mm LEDs. Image of the gonopod was dominated by a purple background and halo concealing the outline of the setae. Medium transparency, prostatic sperm groove on apex somewhat visible.	12V, no resistor required. Shutter: 1 s f-stop: 3.5
5 mm LED, part: RL5-UV0430-400	400	Light composed of a single 5 mm LED. Gonopod image dominated with a purple halo that obscured setae. Several purple glare spots on the gonopod concealed the surface appearance. Lacking transparency.	3.5V and required a resistor. Shutter: 2 s f-stop: 2.8

Ultraviolet light sources were assessed for their ability to capture a fluorescent image of millipede structures. Images were qualitatively assessed by visual examination and favored for a small aperture and a short exposure time. Ultraviolet light-emitting diodes (LEDs) and the modified Canon flash were compared. Since camera flashes typically possess a filter that blocks ultraviolet light, the stock flash was modified to permit short wavelength light between 290 – 360 nm to pass. The Canon 199A has a plastic UV-filter in front of the flash bulb that was easily removed by unscrewing two small screws at the base and unclipping the plastic filter from its housing (Sharboneau 2017). Because strobe bulbs emit broad spectrum light composed of UV and human-visible wavelengths (400 – 700 nm), two filters were placed in front of the bulb element to solely transmit UV light between 290 – 360 nm. The filters were made of Hoya U-340 and S8612 glass (Hoya Corporation, Milpitas, USA) cut to the size of the 199A flash, and are obtained through the Hoya website or the UVIROptics Etsy store that are pre-cut to the 199A filter bezel size (Moon 2017). Several LEDs were tested. The wavelengths varied between 350 – 450 nm, and details about the LED colors and voltages are contained in Table 1. Suppl. material 1 shows the LEDs and the approximate hue of their visible light. A finite number of angles, configurations, and distances of the light sources from the specimen were evaluated. The LED lights were powered by a 12 volt, 1.5 ampere AC to DC adapter, and were continuously illuminated. The 199A flash was connected to the hot shoe of the Canon 6D and was triggered when the shutter was open. Camera operators wore UV-blocking safety glasses and concealed exposed skin to avoid light damage to the eyes and dermal layers.

Results

Images taken with the Canon 199A flash are shown below and results summarized in following descriptions.

Motyxia tularea tularea Xystodesmidae (Fig. 1). (Image of the gonopod, with medial and lateral views.) Variable fluorescence in blue and yellow-green. Acropodite of gonopod translucent, structures visible from behind. Prostatic groove visible from both medial and lateral views. Subbranches of the gonopod clearly visible through translucent cuticle of acropodite. Setal shafts and sockets visible.

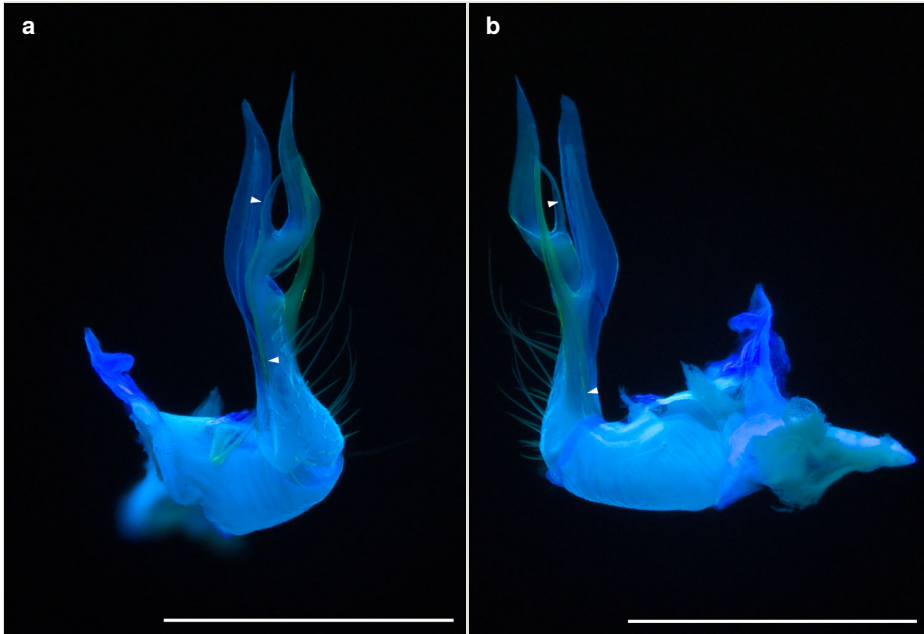


Figure 1.

Fluorescent image of the left gonopod from a male *Motyxia tularea tularea* imaged in 350 nm UV light from a Canon 199A modified flash. Scale bars = 1 mm. Prostatic sperm groove labeled with arrows.

a: Medial view of the gonopod [doi](#)

b: Lateral view of the gonopod [doi](#)

Motyxia sequoiae, Xystodesmidae (Fig. 2a). (Image of the head.) Variable fluorescence in blue and yellow-green. Labral teeth yellow-green and distinct from the head capsule (Fig. 2a, inset). Incisura lateralis dark blue, tentorium arm visible in the center. Setae dark yellow-green, visible against the light blue background. Apical cones of the antenna yellow-green, and contrasted with the blue background.

Siphonacme lyttoni, Siphonophoridae (Fig. 2b). (Image of the head and first nine trunk rings.) Uniform blue fluorescence. The basiconic sensillar pits on antennomere 5 and the beak of the millipede were green in hue and distinct from the uniform blue fluorescence of the cuticle.

Tylobolus uncigerus, Spirobolidae (Fig. 2d). (Image of the anterior and posterior gonopods.) Translucent opal blue fluorescence. Outline sharp and clear. Lacking typical translucence exhibited by polydesmidan gonopods.

Pseudopolydesmus canadensis, Polydesmidae (Figs 2c, 3). (Image of the gonopod and male foreleg.) Variable fluorescence ranging from blue to green. Taxonomically important processes on the gonopod highlighted in blue and green. For example, the pulvillus, coxa, and prefemoral region are blue; and the cannula, medial processes, and spines are green

(Fig. 3a). The sphaerotrichomes on the postfemur, tibia, and tarsus are green and contrast with the leg segments (Fig. 2c, bottom inset). The muscle fibers are a lighter color and visible through the trochanter and prefemur (Fig. 2c, top inset). The purple-blue fluorescence dorsally at the joint between the prefemur and femur may be the protein resilin as a result of its location and distinctive fluorescent color (Fig. 2c).

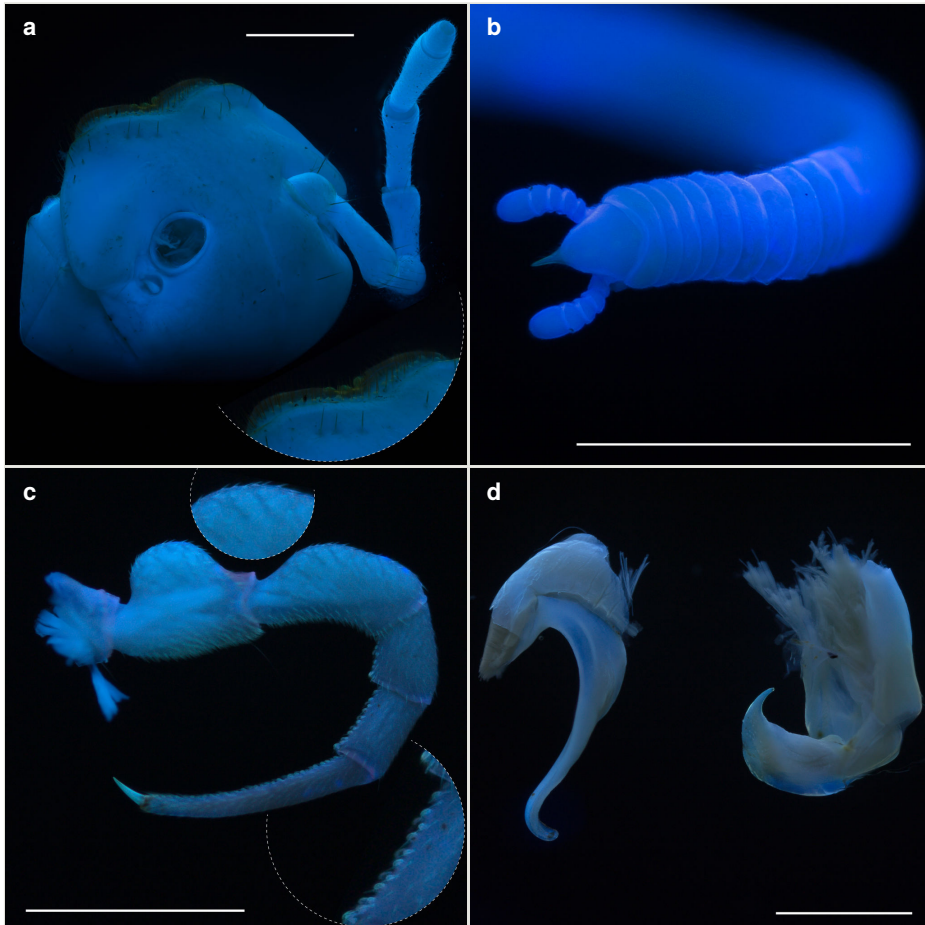


Figure 2.

Fluorescent images of millipedes imaged in 350 nm UV light with a Canon 199A modified flash. Scale bars = 1 mm.

a: Head of *Motyxia sequoiae*, inset: closeup of labral teeth [doi](#)

b: Head and anterior trunk rings of *Siphonacme lyttoni* [doi](#)

c: Foreleg of male *Pseudopolydesmus canadensis*, inset: striated muscles (top) and sphaerotrichomes (bottom) [doi](#)

d: Posterior (left) and anterior (right) gonopods of *Tylobolus uncigerus* [doi](#)

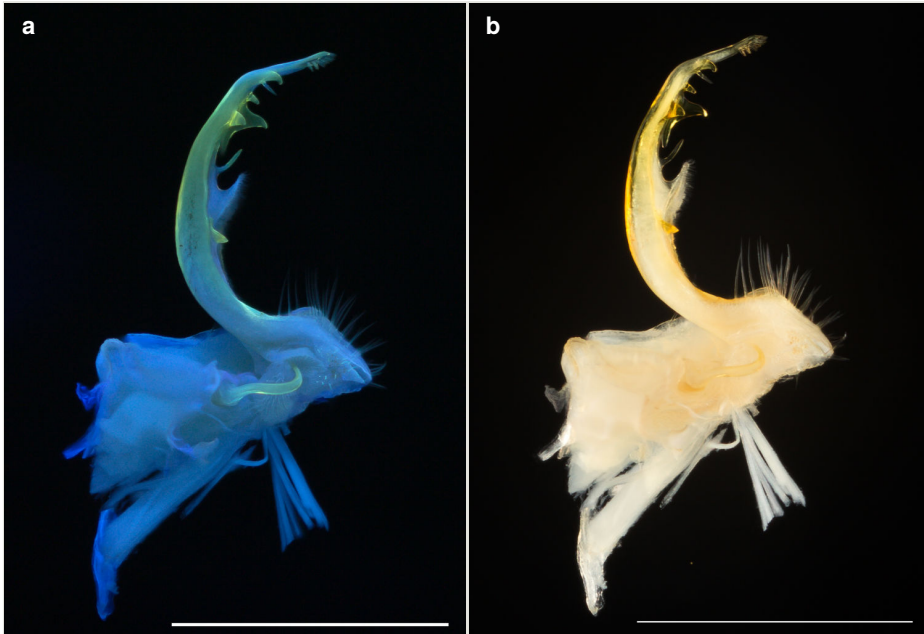


Figure 3.

The left gonopod of a male *Pseudopolydesmus canadensis* imaged in 350 nm UV light from a Canon 199A modified flash and incident visible (white) light. Scale bars = 1 mm.

a: 350 nm UV light from a Canon 199A modified flash [doi](#)

b: Incident visible (white) light [doi](#)

Brachoria sheari, Xystodesmidae (Fig. 4a). (Image of the gonopod.) Variable fluorescence in blue and yellow-green. Prostatic sperm groove visible on the acropodite leading to the apex. The species possesses a more robust gonopod than *P. canadensis* and some transparency is lacking in thickened sections.

The images of the *B. sheari* gonopod photographed with the commercially available UV lights are shown in Figs 4c, d, e, f, 5 and results summarized in Table 1. Two surface-mount device (SMD) LEDs melted and required heatsinks (394 nm and 400/405 nm LEDs). The LEDs generally required large apertures and long exposure times to properly expose the frame with the available light (Table 1). In contrast, the modified Canon 199A flash effectively captured images with small apertures and short exposure times. While filtering the 199A flash did not considerably reduce light intensity, filtering the LED light sources reduced the light intensity significantly that it resulted in an inadequate amount of light to photograph the image. Enlarging the aperture, and lengthening the exposure times in the LED images, to a point where these values were maximized, resulted in extremely grainy photos and errant recording of electrical noise as clusters of red or missing pixels



Figure 4.

Images of the left gonopod from a male *Brachoria sheari* illuminated with different light sources. Scale bar = 1 mm. Prostatic sperm groove labeled with arrows.

a: 350 nm UV light emitted by a Canon 199A modified flash [doi](#)

b: Incident visible (white) light [doi](#)

c: 5 mm 380 nm UV LED radial light [doi](#)

d: 100 mm halo UV light [doi](#)

e: 80 mm halo UV light [doi](#)

f: 5 mm 380 nm UV LED light [doi](#)

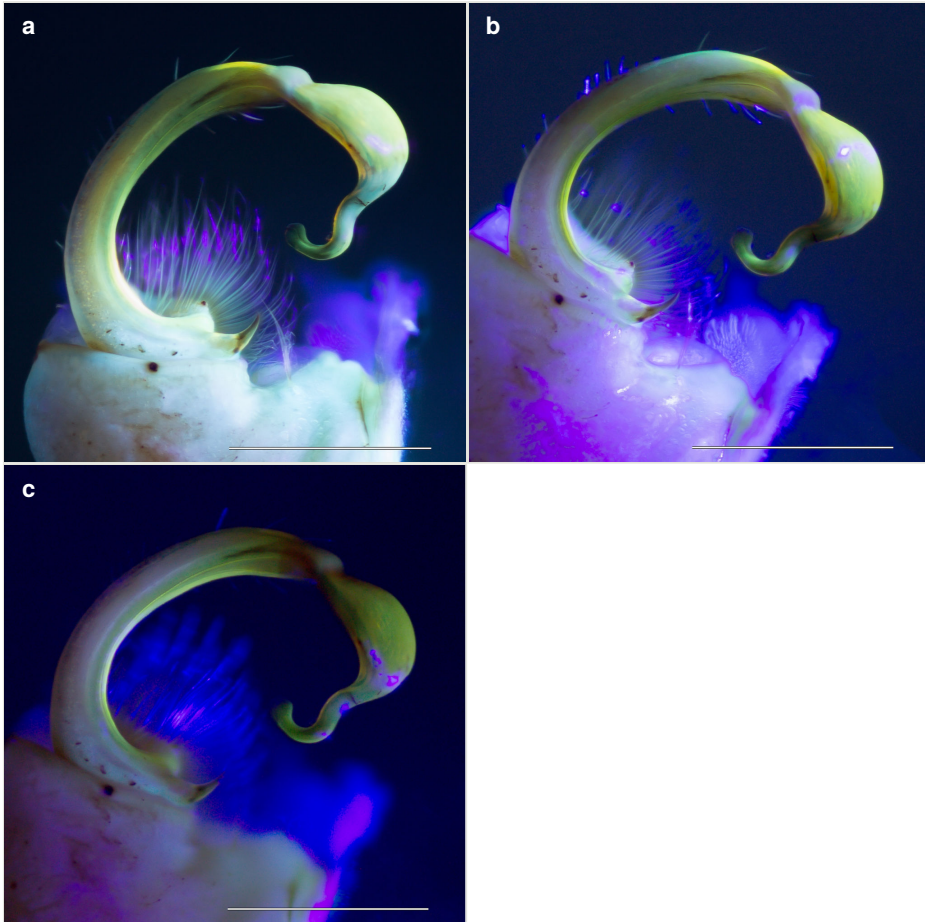


Figure 5.

Images of the left gonopod from a male *Brachoria sheari* illuminated with different light sources. Scale bar = 1 mm.

a: SMD UV LED light [doi](#)

b: 5 mm 400 nm UV light [doi](#)

c: Three-array square SMD LED light [doi](#)

Discussion

The ease of UV induced visible light fluorescence photography is perhaps due to the bright fluorescent emission that is dominant in green wavelengths, to which digital camera sensors are particularly sensitive—green-sensitive elements outnumber blue and red by a factor of two on the Bayer filter mosaics ubiquitous in digital cameras (Bayer 1976). The modified Canon 199A flash, which emitted the lowest and highest intensity wavelength of light, consistently attained high quality images. The LEDs varied in quality, but typically

produced lower quality images affected with bright reflective patches and blue and purple halos surrounding the specimen. The image quality of the Canon 199A flash is likely due to the strobe that emitted an intense pure (narrow spectral peak) UV light that allowed rapid shutter speeds and small apertures, for high depth of field. The 199A flash produced images with a black background and no blue or purple halos as the LEDs did. This is a result of the exclusively short wavelength UV light produced by the 199A (350 nm), of which its stray light was undetectable by the camera due to a UV filter that are normally installed on camera sensors. Light-emitting diodes generally emitted broader spectrum light containing hues of various wavelengths and possessed low intensity, wide-spectrum light. Because UV LEDs emitted some visible light of a longer wavelength than that of the threshold of the sensor filter, it was detected by the camera and produced a glowing blue or purple halo (Figs 4c, d, e, f, 5). The LEDs due to their lower intensities, necessitated long shutter speeds and large apertures to permit additional light to enter the lens due to their relatively lower power. The LEDs that produced good quality images were the 5 mm 380 nm radial LEDs and 80 mm and 100 mm halo lights (Fig. 4c, d, e). These light sources possessed short UV wavelength illumination and/or combined multiple lights.

Every millipede imaged with UV illumination was fluorescent. The Polydesmida, and in particular *Motyxia* and Xystodesmidae, were strongly fluorescent. The images of the gonopod and leg of the polydesmid species *P. canadensis* were sharp and noteworthy because they contain structures that were delineated with different hues. The colors range from blue to green, and the medial processes and pulvillus appeared much sharper compared to the image captured with visible light (Fig. 3a vs Fig. 3b). On the leg of *P. canadensis*, the sphaerotrichomes and striated muscle fibers inside of the prefemur and femur (Fig. 2c, insets) are noticeable, as is the prostatic sperm groove on the gonopodal acropodite (Fig. 3a). In the images of *M. tularea tularea*, different structures are delineated by hue, and the acropodite of the gonopod is translucent allowing structures to be viewed through the surface (Fig. 1). For example in *M. tularea tularea*, the selenomere and lateral subbranch of the prefemoral process are visible from behind the “B” process and are visible at both the lateral and medial views (terminology sensu Shelley 1997). The gonopods of *T. uncigerus*, a spirobolid millipede, fluoresce a light opalescent blue (Fig. 2d). While the edges are well-defined, the translucence is reduced compared to the polydesmidan representatives. The medial processes of *P. canadensis*, acropodal apices of *Motyxia* species, beak of *S. lytoni*, and the labral teeth of *M. sequoiae* are heavily calcified. These heavily calcified structures, lacking muscle and lipids below the surface, are most easily imaged with this photographic technique.

Conclusions

Fluorescent imaging may provide a useful and inexpensive method for capturing high quality images for millipede taxonomy. Using the endogenous fluorescence of millipedes, subtle structures such as the prostatic sperm groove are noticeable and ultraviolet illumination preserves transparency such that small spines and processes—even muscle fibers in some cases—can be seen through cuticle that may otherwise obscure it. The

technique allows examination of fine shapes from different angles, more than may be possible with visible light or scanning electron micrography.

Though many research institutions possess confocal microscopes, and these instruments have been successfully demonstrated to capture arthropod cuticle morphology, there may be an hourly charge for beam time and a queue if the instrument is frequently used. This study concludes that four portable inexpensive ultraviolet light sources work well for fluorescent imaging. (1) The two circular halo lights and the 380 nm 5-mm LEDs arranged in a radial pattern generated sharp evenly fluorescent images (Fig. 4c, d, e; Suppl. material 1). These light source provide a low-cost solution for ultraviolet induced fluorescent imaging that can be retrofitted to most preexisting imaging systems. (2) If researchers possess a dSLR camera and focus-stacking software, the Canon 199A flash may be the better choice because the light generated is bright and pure, and higher f-stops and shutter speeds can be implemented (Figs 1, 2, 3a, 4a). Future directions to refine this technique include filtering the UV light to match the maximum absorption wavelength of taxa with different fluorescent colors, mixing visible white light with UV illumination, and increasing the number of LEDs to maximize the intensity of the relatively weak illumination. Furthermore, UV induced fluorescent photography of live millipedes has been accomplished for a few taxa, including one—*Thrinaphe hargerii* Shelley, 1993—that has a metatergal color pattern that is only visible under short wavelength UV light.

Acknowledgements

Petra Sierwald provided comments and revisions on previous versions of the manuscript.

Funding program

This study was supported by a NSF Systematics and Biodiversity Science Advancing Revisionary Taxonomy and Systematics (ARTS) award to P. Marek (DEB# 1655635). Supplemental funding was provided by a Virginia Tech USDA NIFA Hatch Project (VA-160028).

Conflicts of interest

The author states there is no conflict of interest.

References

- Bayer BE (1976) Color imaging array. Google Patents
- Johnsen S (2012) *The Optics of Life*. Princeton University Press, Princeton, 336 pp. <https://doi.org/10.1515/9781400840663>

- Kuse M, Yanagi M, Tanaka E, Tani N, Nishikawa T (2010) Identification of a fluorescent compound in the cuticle of the train millipede *Parafontaria laminata armigera*. *Bioscience, biotechnology, and biochemistry* 74 (11): 2307-2309. <https://doi.org/10.1271/bbb.100171>
- Kuse M, Kanakubo A, Suwan S, Koga K, Isobe M, Shimomura O (2001) 7,8-Dihydropterin-6-carboxylic acid as light emitter of luminous millipede, *Luminodesmus sequoiae*. *Bioorganic & Medicinal Chemistry Letters* 11 (8): 1037-1040. [https://doi.org/10.1016/s0960-894x\(01\)00122-6](https://doi.org/10.1016/s0960-894x(01)00122-6)
- Lee S, Brown R, Monroe W (2009) Use of confocal laser scanning microscopy in systematics of insects with a comparison of fluorescence from different stains. *Systematic Entomology* 34 (1): 10-14. <https://doi.org/10.1111/j.1365-3113.2008.00451.x>
- Marek P, Moore W (2015) Discovery of a glowing millipede in California and the gradual evolution of bioluminescence in Diplopoda. *Proceedings of the National Academy of Sciences* 112 (20): 6419-6424. <https://doi.org/10.1073/pnas.1500014112>
- Marek P, Papaj D, Yeager J, Molina S, Moore W (2011) Bioluminescent aposematism in millipedes. *Current Biology* 21 (18): R680-R681. <https://doi.org/10.1016/j.cub.2011.08.012>
- Marshall J, Johnsen S (2017) Fluorescence as a means of colour signal enhancement. *Philosophical Transactions of the Royal Society B: Biological Sciences* 372 (1724): 20160335. <https://doi.org/10.1098/rstb.2016.0335>
- Means J, Francis E, Lane A, Marek P (2015) A general methodology for collecting and preserving xystodesmid and other large millipedes for biodiversity research. *Biodiversity Data Journal* 3: e5665. <https://doi.org/10.3897/bdj.3.e5665>
- Moon I (2017) UVIROPTICS: Specialty infrared and ultraviolet camera filters. www.etsy.com/uviroptics. Accessed on: 2017-6-28.
- Needham AE (1968) Integumental Pigments of the Millipede, *Polydesmus angustus* (Latzel). *Nature* 217 (5132): 975-977. <https://doi.org/10.1038/217975a0>
- Oba Y, Branham MA, Fukatsu T (2011) The terrestrial bioluminescent animals of Japan. *Zoological science* 28 (11): 771-789. <https://doi.org/10.2108/zsj.28.771>
- Oba Y, Stevani C, Oliveira A, Tsarkova A, Chepurnykh T, Yampolsky I (2017) Selected least studied but not forgotten bioluminescent systems. *Photochemistry and Photobiology* 93 (2): 405-415. <https://doi.org/10.1111/php.12704>
- Pearsons K, Mikó I, Tooker J (2017) The cyanide gland of the greenhouse millipede, *Oxidus gracilis* (Polydesmida: Paradoxosomatidae). *Research Ideas and Outcomes* 3: e12249. <https://doi.org/10.3897/rio.3.e12249>
- Rosenberg J, Meyer-Rochow VB (2009) Luminescent myriapoda: a brief review. In: Meyer-Rochow VB (Ed.) *Bioluminescence in Focus: A Collection of Illuminating Essays*. Research Signpost, Trivandrum, India, 385 pp. [ISBN 978-81-308-0357-9].
- Sharboneau E (2017) UV Blacklight Photography Tutorial (Ultraviolet-Induced Visible Fluorescence). <http://photoextremist.com/ultraviolet-induced-visible-fluorescence-photography-tutorial>. Accessed on: 2017-6-28.
- Shelley R (1997) A re-evaluation of the milliped genus *Motyxia* Chamberlin, with a re-diagnosis of the tribe Xystocheirini and remarks on the bioluminescence (Polydesmida: Xystodesmidae). *Insecta Mundi* 11: 331-351. URL: <http://digitalcommons.unl.edu/cgi/viewcontent.cgi?article=1279&context=insectamundi>
- Shimomura O (2006) *Bioluminescence - Chemical Principles and Methods*. World Scientific, Hackensack. <https://doi.org/10.1142/9789812773647>

Supplementary material

Suppl. material 1: Supplementary figure S1 [doi](#)

Authors: Marek, Paul

Data type: images

Brief description: LED lights assessed in this study. A. 5 mm 380 nm LED light; B. 5 mm LED radial light; C. SMD LED starlight; D. SMD triple UV light; E. SMD single LED light; F. Canon 199A 350 nm UV light; G. 5 mm LED radial light; H. 80 mm halo UV light; I. 100 mm halo UV light.

Filename: SupplementalFigure_S1.jpg - [Download file](#) (2.09 MB)